# CLOSED CLUSTERS APPROACH TO GRAPHENE

Ilja I. Taljanskij

*Department for Theoretical Physics, Ivan Franko National University of Lviv;*
*current address[†]: Rudolf-Breitscheid-Strasse 39, 23968 Wismar, Germany*

The Closed Cluster method (CC method) is applied to find solutions for various calculation problems of the energy band structure of graphene. The essence of the CC method consists in the addition of closing bonds between edge atoms to the usual cluster method in order to eliminate the "dangling" bonds on the edges of the cluster. We study the cases of an "infinite" layer of graphene as well as nanoribbons, nanotubes and bilayer graphene. Results for these cases are in agreement with what was obtained using other methods (tight binding approximation and others). Using the CC method, we also study the problem of point defects in graphene and obtain the distortion of the energy spectrum. The energy spectrum of the layer $C_{1-x}Si_x$ ($0 \leq x \leq 1$) is found as well as the dependence of the energy gap on the concentration of silicon. We show that the energy band structure of $C_{1-x}Si_x$ looks like a tunnel transition. Wave functions of graphene in the symmetry points of Brillouin zone are also obtained.

**Key words:** graphene, energy band structure, point defects, nanostructures.

## I. INTRODUCTION

Studies of various properties of graphene and its applications have attracted much attention in the last years, as is well-known [1]. In this paper, we propose an approach based on the use of closed clusters (CC) to calculate the energy band structure of graphene. We developed this approach earlier in application to the one-dimensional and three-dimensional crystals with diamond structures [2]. The essence of the CC approach is to bring together all bonds of atoms which are located on the edge of a cluster in order to eliminate the "dangling" bonds. This approach is found to be especially useful for calculation of the energy spectrum of crystals with point defects, such as vacancies or impurity atoms. The simplest and most widespread approach to calculate such impurity states is known to be the effective mass method. This approximation works sufficiently well in cases of impurity levels being located along the borders of the energy zones. However, it is inapplicable to the description of the so-called "deep levels", which lie far from the zone borders [3]. One of the methods used for those levels is the cluster approach, in which a group of atoms — the cluster — is mentally picked from a crystal lattice.

This cluster is considered a separate "molecule" and for its calculation the usual quantum chemistry methods are applied. The advantage of the clusters approach is its applicability for modelling real situations of impurity atoms and — if necessary — taking into consideration a possible distortion of the crystal lattice.

However, the usual cluster approach has a deficiency. If the "infinity" crystal is substituted with a group of atoms, a problem with atoms lying on the edge of the cluster arises. The presence of such atoms with torn bonds distorts the energy spectrum of the crystal. This distortion can be diminished by increasing the size of the cluster, but the approximation to the exact value is very slow.

This deficiency can instead be removed by connecting the torn bonds with each other and hereby closing them. A similar procedure, the so-called "periodical boundary conditions", is applied in studying the energy spectrum of the infinite ideal crystals. The special feature of our approach is the application of the closing procedure of these bonds to small clusters to study crystals with distorted regularity properties (such as impurity, edges and other). In this paper, the CC approach is applied to graphene, a relatively new material with numerous unique properties [4]. In Section II, the fundamental idea of the CC approach is presented as well as the rules for the construction of diagrams corresponding to the various clusters. In Section III, examples of building Hamiltonian matrices and solutions for the secular equations in the case of periodical structures without edges and defects are given. The aim of this section is to test our approach by comparising the results with those obtained using other methods. In Section IV, the CC approach is applied to bilayer graphene. In Section V, we present wave functions at symmetry points of the Brillouin zone. In Section VI we study nanoribbons and nanotubes by means of closed clusters. Section VII, contains the calculations of the graphene energy spectrum in the presence of impurity. Finally, in Section VIII we study the energy band structure of the hypothetic monoatomic layer $C_{1-x}Si_x$ ($0 \leq x \leq 1$). Section IX concludes with a discussion of the obtained results and, describes a possibility for making the approach more precise as well as the application of the CC approach to other problems.

---

## II. THE ESSENCE OF THE CC APPROACH AND A RULE FOR CONSTRUCTING THE DIAGRAMS

By the term a "closed cluster" we mean a group of $N$ atoms which reflects the structure of the crystal and furthermore the atom bonds which are present within the group; at the same time, the torn bonds are absent. A similar procedure of closing the bonds known as "periodical boundary conditions" is often used in one-dimensional atom chains when atom $N+1$ is identical to the first one. Such a procedure is also possible for 3D-systems, but is rarely applied here, since closing a 3D cluster is much more difficult. In 2D cases, however, closing can be realized very easily — therefore, the application of the CC approach to graphene and other 2D structures seems to be very effective.

While constructing clusters corresponding to graphene, one must start out from its crystal structure. The latter is well-known, a hexagonal layer which is formed by two sublattices, here A and B [5]. The simplest unclosed cluster corresponding to such a structure is shown in Fig. 1(a).

The main idea of the closed cluster approach is the necessity of closing the torn bonds shown in Fig. 1(a) in the way shown in Fig. 1(b). In the case of an endless graphene layer, the structure of the lattice requires the following rules regarding the construction of a closed cluster with approximation of the nearest neighbors.
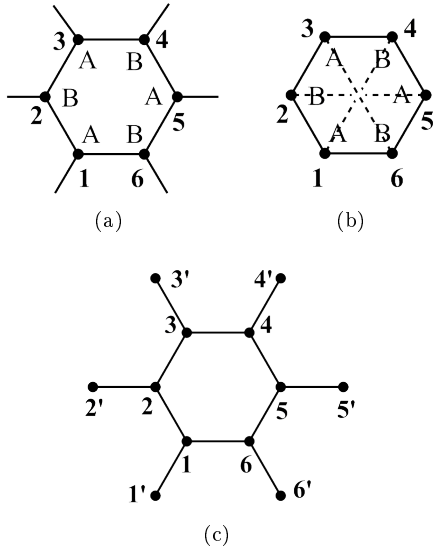


(a)              (b)



(c)

Fig. 1. The most simple clusters of the graphene lattice
(a) unclosed cluster $N = 6$
(b) closed cluster $N = 6$
(c) cluster surrounded by neighbor atoms
dashed line: closing bonds
continuous line: real bonds in graphene lattice

- **Rule 1.** Each atom of sublattice A is bonded with three atoms of sublattice B and vice versa.

- **Rule 2.** All real and closing bonds have the same energy levels.

- **Rule 3.** The number of atoms in a cluster $N$ must be divisible by six.

The last rule is explained in detail in Section V.

All three rules in fact are satisfied within the construction in Fig. 1(b), although the second rule seems to be broken at first sight: for example, the closing bond between atoms 1 and 4 looks different from that between 1–2 or 1–6, since atom 4 is further away from 1. However, it must be kept in mind that the bond 1–4 is not a real bond. In contrast to Fig. 1(c), the closed cluster 1(b) must be understood as a diagram or graph, which makes it easier to obtain the Hamiltonian matrix. Furthermore, if these Hamiltonian matrix elements corresponding to the closing bonds are chosen to be the same as for existing bonds, then the "interaction" between atoms like 1 and 4 in 1(b) in fact describes the interaction between 1 and $1'$ in 1(c), the latter of which is absent from cluster $N = 6$.

It must be noted that the numbers of atoms in sublattices A and B have to be equal, as closing bonds are only possible between atoms of different sublattices. For example, in cluster 1(b) it is only possible to close the bonds of atom 1 with atom 4, but not with 3 or 5. This restriction is necessary to satisfy Rule 1.

We also note that energy values obtained from the solution of secular equations are independent from the choice of the cluster in the case of an "infinite" ideal lattice, but are only dependent on the number $N$. They are also independent of the numeration of the atoms, since changes in numeration only cause determinant permutations.

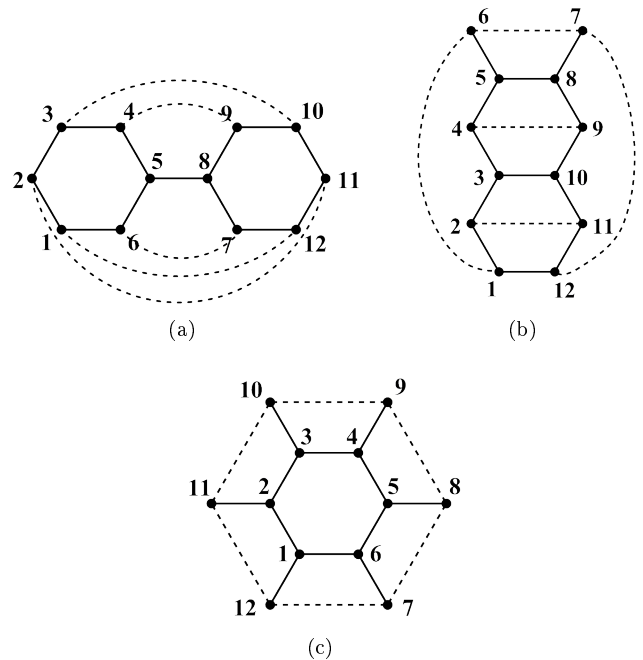Fig. 2 shows some of the possible clusters with $N = 12$ with dissimilar ways of closing.



(a)                          (b)



(c)

Fig. 2. Examples of closed clusters for $N = 12$

To conclude this section, we note, that the name "closed cluster", which we use, is different from the term

"closed walk" used in graph theory [6]. For example, the cluster shown in Fig. 1(a) is a "closed walk", but not a closed cluster — the latter is shown in Fig. 1(b).

One definition of a closed cluster can be given as a cluster where each atom is linked to the same number of neighboring atoms as in the corresponding crystal.

## III. BUILDING A HAMILTONIAN MATRIX AND SOLUTION OF SECULAR EQUATIONS

The basic idea underlying the CC approach is the same as in the usual molecular orbital approach (MO) [7]. In particular, this is the representation of the wave function of the cluster $\Psi(\underline{r})$ as a linear combination of the wave functions of the atoms

$$\Psi(\mathbf{r}) = \sum_{n=1}^{N} c_n \varphi(\mathbf{r} - \mathbf{a}_n). \qquad (1)$$

Functions $\varphi$ in graphene are $|p_z\rangle$ — orbitals of carbon atoms, with axis z being perpendicular to the layer. We designate wave functions along and opposed to this axis as "+" and "−".

The standard procedure of obtaining secular equations leads to a system of linear equations which help to find the coefficients $c_n$ in

$$\sum_{n=1}^{N} M_{mn} c_n = 0, \qquad m = 1, 2, \ldots, N, \qquad (2)$$

where

$$M_{mn} = \varepsilon \delta_{mn} + (1 - \delta_{mn})\eta_{mn}, \qquad (3)$$

$$\delta_{mn} = \begin{cases} 1, m = n \\ 0, m \neq n, \end{cases}$$

$$\eta_{mn} = \begin{cases} 1, \text{if atom m is bound with atom n} \\ 0, \text{if atom m is not bound with atom n}, \end{cases}$$

$$\varepsilon = \frac{E - E_0}{\gamma_0}$$

with

$E$ — energy of an electron

$E_0$ — energy of an electron in the $|2p_z\rangle$ state in an isolated carbon atom. We use $E_0 = 0$

and $-\gamma_0$ — the transfer integral between neighboring atoms with wave functions with the same sign, $\gamma_0 > 0$.

The problem of calculating the corresponding values of energy $\varepsilon$ (in $\gamma_0$ units) is then reduced to solving the secular equation

$$\det M_{mn} = 0. \qquad (4)$$

Now we consider some examples of applications of the approach. We begin with the simplest closed cluster $N = 6$, which is shown in Fig. 1(b). The secular equation (4) has the form (empty matrix cells standing here and further for zeroes):

$$D_6 = \begin{vmatrix} \varepsilon & 1 & 1 & & & 1 \\ 1 & \varepsilon & 1 & & 1 & \\ & 1 & \varepsilon & 1 & & 1 \\ 1 & & 1 & \varepsilon & 1 & \\ & 1 & & 1 & \varepsilon & 1 \\ 1 & & 1 & & 1 & \varepsilon \end{vmatrix} = 0. \qquad (5)$$

Calculating the determinant (5) leads to the following equation for finding $\varepsilon$:

$$\varepsilon^4(\varepsilon^2 - 9) = 0. \qquad (6)$$

The solutions of (6) $\pm 3, 0, 0, 0, 0$ are exactly those energy values at bottom, top and Dirac points of two energy bands, which are obtained from a tight binding and nearest neighbor approximations [5].

The fact, that the CC approach provides exact values of energy band boundaries already at a minimal cluster size is very important in the calculation of the energy of impurity states, as the energy of such states counted from the bands' boundaries.

Let us consider the next example with $N = 12$. If we proceed from the clusters from Fig. 2, then the secular equation has the form:

$$D_{12} = \begin{vmatrix} \varepsilon & 1 & & & & & 1 & & & & & 1 \\ 1 & \varepsilon & 1 & & & & & & & & 1 & \\ & 1 & \varepsilon & 1 & & & & & & 1 & & \\ & & 1 & \varepsilon & 1 & & & & 1 & & & \\ & & & 1 & \varepsilon & 1 & 1 & & & & & \\ 1 & & & & 1 & \varepsilon & 1 & & & & & \\ & & & & & 1 & \varepsilon & 1 & & & & 1 \\ & & & & 1 & & 1 & \varepsilon & 1 & & & \\ & 1 & & & & & & 1 & \varepsilon & 1 & & \\ & & 1 & & & & & & 1 & \varepsilon & 1 & \\ 1 & & & & & & & & & 1 & \varepsilon & 1 \\ 1 & & & & & & 1 & & & & 1 & \varepsilon \end{vmatrix} = 0. \qquad (7)$$

The solution of equation (7) is given by the following values of energy $\varepsilon$: $\pm 3, \pm 2, \pm 2, \pm 1, 0, 0, 0, 0$.

The determinant of cluster $N = 24$ has a form which is analogous to (7) $D_{12}$. The obtained energy values are shown in Table 1.

The main conclusion which may be drawn from the comparison of cases $N = 6$, 12 and 24 is the fact that the energy values of the bottoms and tops of the lower $(-3, 0)$ and upper band $(0, 3)$ are equal in each case; therefore, they are independent of the cluster size. With the growth of the cluster size, new energy levels arise; however, previous levels remain the same.

Each energy value in Table 1 corresponds to some point of the Brillouin zone. More in-detail discussion on that issue is presented in Sec. V. At this point we just briefly discuss the fourfold degeneration of level $\varepsilon = 0$ at all $N$.

At first glance it does not seem to be in accordance with $\varepsilon$ being 0 at six corners of the Brillouin zone (points $K_1$, $K_2$, ..., $K_6$ in Fig. 3).

Table 1. Electron energy values with varying numbers of atoms in the cluster

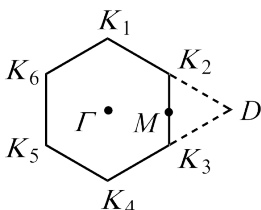| $N$ | Energy | | | | | | | | | | | | | |
|---|---|---|---|---|---|---|---|---|---|---|---|---|---|---|
| 6 | $\pm 3$ | | | | | | | | | | 0 | 0 | 0 | 0 |
| 12 | $\pm 3$ | | | $\pm 2$ | $\pm 2$ | | $\pm 1$ | | | | 0 | 0 | 0 | 0 |
| 24 | $\pm 3$ | $\pm(\sqrt{3}+1)$ | $\pm(\sqrt{3}+1)$ | $\pm 2$ | $\pm 2$ | $\pm 1$ | $\pm 1$ | $\pm 1$ | $\pm(\sqrt{3}-1)$ | $\pm(\sqrt{3}-1)$ | 0 | 0 | 0 | 0 |



Fig. 3. Brillouin zone of graphene [5]

However, it must be kept in mind that only two of these six points, $K_1$ and $K_2$ for example, belong to the first Brillouin zone, others belonging to the next zones. The twofold degeneration at points $K_1$ and $K_2$ is what leads to fourfold degeneration of the level $\varepsilon = 0$.

To conclude this section, it should be noted that the rules for diagram construction formulated in sec. III do not require these diagrams to be plane. Therefore, they also can be applied to nanotubes as well as spherical surfaces (fullerene). A stratified cluster can also be used. For example, the diagram in Fig. 2(a) can be rearranged to a hexahedron without breaking the bonds. The application for the space diagram is useful for studying many-layer graphene. In the next section, we use a three-dimensional diagram to study bilayer graphene.

## IV. BILAYER GRAPHENE

For $N = 12$, the 3D closed cluster corresponding to bilayer graphene is shown in Fig. 4. In addition to the closing bonds within the layers (energy $\gamma_0$), also the bonds describing the interactions between those layers (energy $\gamma_1$ in $\gamma_0$-units) are present in the cluster.

Note, that Fig. 4 does not show the displacement of the upper layer towards the lower, since this Figure doesn't reproduce a real atomic structure, but is solely a diagram which is used for building a Hamiltonian matrix.



——— real bonds within the layers $\gamma_0$,
- - - - - closing bonds within the layers $\gamma_0$,
ıııııııı bonds between layers $\gamma_1$.
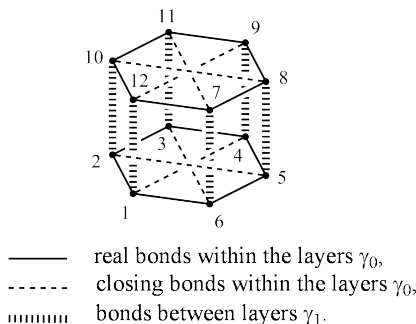
Fig. 4. Cluster $N = 12$ for bilayer graphene

The secular equation corresponding to Fig. 4 has the form

$$D_{12}^{(2)} = \begin{vmatrix} \varepsilon & 1 & & 1 & & 1 & & & & & & \gamma_1 \\ 1 & \varepsilon & 1 & & 1 & & & & & & \gamma_1 & \\ & 1 & \varepsilon & 1 & & 1 & & & & \gamma_1 & & \\ 1 & & 1 & \varepsilon & 1 & & & & \gamma_1 & & & \\ & 1 & & 1 & \varepsilon & 1 & & \gamma_1 & & & & \\ 1 & & 1 & & 1 & \varepsilon & \gamma_1 & & & & & \\ & & & & & \gamma_1 & \varepsilon & 1 & & 1 & & 1 \\ & & & & \gamma_1 & & 1 & \varepsilon & 1 & & 1 & \\ & & & \gamma_1 & & & & 1 & \varepsilon & 1 & & 1 \\ & & \gamma_1 & & & & 1 & & 1 & \varepsilon & 1 & \\ & \gamma_1 & & & & & & 1 & & 1 & \varepsilon & 1 \\ \gamma_1 & & & & & & 1 & & 1 & & 1 & \varepsilon \end{vmatrix} = 0. \quad (8)$$

Solving equation (8) leads to following energy levels:

$$\varepsilon = \pm(3 + \gamma_1), \pm(3 - \gamma_1), \pm\gamma_1, \pm\gamma_1, \pm\gamma_1, \pm\gamma_1. \quad (9)$$

The main result that ensues from (9) is that there is an energy gap $\varepsilon_g = 2\gamma$. The presence of this gap in bilayer graphene is a fact discussed in many papers [8, 9]. In the model which we are using, the energy gap is caused by the interaction between the layers and disappears if we set $\gamma_1=0$.

## V. WAVE FUNCTIONS

Within our considered model, the cluster wave functions are determined by the totality of coefficients $c_n$, according to (1). To obtain the latter, one must solve the system of equations (2) under defined energy values $\varepsilon$. For $\varepsilon = 3$ and $\varepsilon = -3$ the result is obvious and shown in Table 2. Let us now consider the cases $\varepsilon = \pm 1$ and $\varepsilon = 0$ in more detail. The latter is most interesting, since at this point the valence band meets the conduction band.

As an example, let us consider the cluster $N = 12$, which is shown in Fig. 2(b), but with a different atoms numbering (Fig. 5).
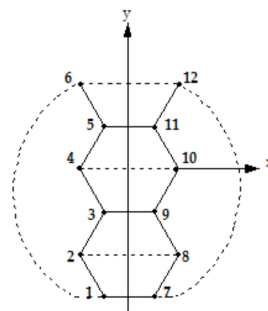


Fig. 5. Cluster $N = 12$ for the calculation of graphene wave functions

To determine the coefficients $c_1, c_2, \ldots, c_{12}$ in (2), we must solve a system of twelve linear equations. For the cluster in Fig. 5, it has the form

$$\begin{cases}
(1) & \varepsilon c_1 + c_2 + c_6 + c_7 = 0 \\
(2) & c_1 + \varepsilon c_2 + c_3 + c_8 = 0 \\
(3) & c_2 + \varepsilon c_3 + c_4 + c_9 = 0 \\
(4) & c_3 + \varepsilon c_4 + c_5 + c_{10} = 0 \\
(5) & c_4 + \varepsilon c_5 + c_6 + c_{11} = 0 \\
(6) & c_1 + c_5 + \varepsilon c_6 + c_{12} = 0 \\
(7) & c_1 + \varepsilon c_7 + c_8 + c_{12} = 0 \\
(8) & c_2 + c_7 + \varepsilon c_8 + c_9 = 0 \\
(9) & c_3 + c_8 + \varepsilon c_9 + c_{10} = 0 \\
(10) & c_4 + c_9 + \varepsilon c_{10} + c_{11} = 0 \\
(11) & c_5 + c_{10} + \varepsilon c_{11} + c_{12} = 0 \\
(12) & c_6 + c_7 + c_{11} + \varepsilon c_{12} = 0
\end{cases} \qquad (10)$$

As we can see from Fig. 5, our cluster is reflection-symmetric in the axes $y$ and $x$, due to the closing bonds 1–6 and 7–12. Hence, wave functions must be symmetric $(S_x, S_y)$ or antisymmetric $(A_x A_y)$ to the reflection in the $x$ and $y$ axis. Altogether there are four possible symmetries of wave functions: $S_x S_y, S_x A_y, A_x S_y$ and $A_x A_y$.

First we consider the $S_x S_y$ case. The following relations among the coefficients must be satisfied:

$$S_x S_y : \begin{cases}
c_1 = c_7 \\
c_2 = c_6 = c_8 = c_{12} \\
c_3 = c_5 = c_9 = c_{11} \\
c_4 = c_{10}
\end{cases} \qquad (11)$$

Then the task is to solve just four equations instead of twelve.

If we take (11), the equations have the form

$$S_x S_y : \begin{cases}
1. (\varepsilon + 1)c_1 + 2c_2 & = 0 \\
2. \quad c_1 + (\varepsilon + 1)c_2 + c_3 & = 0 \\
3. \qquad c_2 + (\varepsilon + 1)c_3 + c_4 & = 0 \\
4. \qquad\quad 2c_3 + (\varepsilon + 1)c_4 & = 0
\end{cases} \qquad (12)$$

The determinant of (12) has to be zero and therefore we obtain

$$S_x S_y : \varepsilon = -3, -2, 0, 1. \qquad (13)$$

In other symmetry cases we have

$$S_x A_y : \begin{cases}
c_1 = -c_7, \\
c_2 = c_6 = -c_8 = -c_{12}, \\
c_3 = c_5 = -c_9 = -c_{11}, \\
c_4 = -c_{10}
\end{cases} \qquad (14)$$

$$A_x S_y : \begin{cases}
c_1 = c_7 = 0, \\
c_2 = -c_6 = c_8 = -c_{12}, \\
c_3 = -c_5 = c_9 = -c_{11}, \\
c_4 = c_{10} = 0
\end{cases} \qquad (15)$$

$$A_x A_y : \begin{cases}
c_1 = c_7 = 0, \\
c_2 = -c_6 = -c_8 = c_{12}, \\
c_3 = -c_5 = -c_9 = c_{11}, \\
c_4 = c_{10} = 0
\end{cases} \qquad (16)$$

In the latter two cases, there is $c_1 = c_4 = c_7 = c_{10} = 0$ due to the antisymmetry to axis $x$ $(A_x)$. Therefore, only two equations remain in each case, namely those of the coefficients $c_2$ and $c_3$, and consequently, only two values of energy for each $A_x S_y$ and $A_x A_y$.

The energy levels for various symmetries are shown in Table 2; Table 3 shows the values of the coefficients $c_1, c_2, \ldots, c_{12}$. These coefficient values are obtained by solving the system of equations like (12) and analogous systems for other symmetries for the energies $\varepsilon = 0, \pm 1, \pm 3$. The set of these coefficients determines the wave functions for various symmetries within our considered model. Tables 2 and 3 also show the Brillouin zone symmetry points, which can also be seen in Fig. 3.

For the purpose of illustration, one can represent these functions graphically by extending the cluster over the whole graphene layer. In the case $\varepsilon = \pm 1$, the functions coincide with those in [5]. For the case $\varepsilon = 0$, wave functions for various symmetries are shown in Fig. 6.
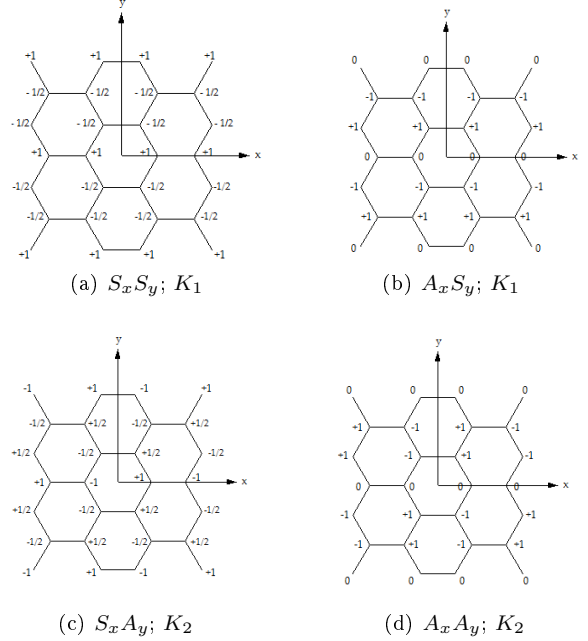


(a) $S_x S_y; K_1$



(b) $A_x S_y; K_1$



(c) $S_x A_y; K_2$



(d) $A_x A_y; K_2$

Fig. 6. Wave functions of graphene various symmetries at the points $K$. The data is taken from Table 3

From Fig. 6 it is easy to see that in cases 6(a) and 6(b) the wave functions are plane waves with $\lambda = \frac{3}{2}a$, where $a$ is the length of the vector connecting the nearest neighbors of atoms A and B. The fronts of these waves are parallel to axis $x$, which means that the wave vector $\boldsymbol{k}$ is directed along axis $y$.

The length of the wave vector of these waves $k = \frac{2\pi}{\lambda} = \frac{4\pi}{3a}$ coincides with the length of $\boldsymbol{k}$ of Brillouin zone point $K_1$ (Fig. 3) — thus, Figures 6(a) and 6(b) show the wave functions at point $K_1$. In cases 6(c) and 6(d) one can easily see that the fronts of the wave of each sublattice are at an $120°$ angle to the axis $x$. Therefore, the waves, vectors are directed at a $30°$ angle to axis $x$, that is the point $K_2$ in Fig. 3. The length of these waves is also $\frac{3}{2}a$. As a consequence, Fig 6(c) and Fig. 6(d) show the wave functions at point $K_2$.

The fact that all four wave functions shown in Fig. 6 correspond to the energy $\varepsilon = 0$ can be directly deduced from the form of these functions. Namely, the total energy of the interactions of the atoms with their respective nearest neighbors is equal to zero, taking into consideration the values and signs of $c_n$ from Fig. 6.

In Fig. 6 it is also evident, that those structure elements which are periodically repeated within the wave functions at $\varepsilon = 0$ are triplets of atoms: $1, -1, 0$ (Fig. 6(b)), $1, -\frac{1}{2}, -\frac{1}{2}$ (Fig. 6(a)) etc. Consequently, the energy value $\varepsilon = 0$ is only

Table 2. Energy levels of cluster $N = 12$ corresponding to various symmetries of wave functions

| Symmety ＼ Energy level | $\varepsilon_1$ | $\varepsilon_2$ | $\varepsilon_3$ | $\varepsilon_4$ | $\varepsilon_5$ | $\varepsilon_6$ | $\varepsilon_7$ | $\varepsilon_8$ | $\varepsilon_9$ | $\varepsilon_{10}$ | $\varepsilon_{11}$ | $\varepsilon_{12}$ |
|---|---|---|---|---|---|---|---|---|---|---|---|---|
| $S_x S_y$ | -3 | -2 | | | 0 | | | | 1 | | | |
| $S_x Y_y$ | | | | -1 | | 0 | | | | | 2 | 3 |
| $A_x S_y$ | | | -2 | | | | 0 | | | | | |
| $A_x A_y$ | | | | | | | | 0 | | 2 | | |
| Point of BZ | $\Gamma$ | | | $M-0$ | $K_1$ | $K_2$ | $K_1$ | $K_2$ | $M+0$ | | | $D$ |

Table 3. Wave functions at the symmetry points of the Brillouin zone

| $c_n$ ＼ Energy | $-3$ | $-1$ | $0$ | $0$ | $0$ | $0$ | $1$ | $3$ |
|---|---|---|---|---|---|---|---|---|
| $c_1$ | 1 | 1 | 1 | 1 | 0 | 0 | 1 | 1 |
| $c_2$ | 1 | 1 | $-1/2$ | $-1/2$ | 1 | 1 | $-1$ | $-1$ |
| $c_3$ | 1 | 1 | $-1/2$ | $-1/2$ | $-1$ | 1 | 1 | 1 |
| $c_4$ | 1 | 1 | 1 | $-1$ | 0 | 0 | $-1$ | $-1$ |
| $c_5$ | 1 | 1 | $-1/2$ | $-1/2$ | 1 | $-1$ | 1 | 1 |
| $c_6$ | 1 | 1 | $-1/2$ | $1/2$ | $-1$ | $-1$ | $-1$ | $-1$ |
| $c_7$ | 1 | $-1$ | 1 | $-1$ | 0 | 0 | 1 | $-1$ |
| $c_8$ | 1 | $-1$ | $-1/2$ | $1/2$ | 1 | $-1$ | $-1$ | 1 |
| $c_9$ | 1 | $-1$ | $-1/2$ | $1/2$ | $-1$ | $-1$ | 1 | $-1$ |
| $c_{10}$ | 1 | $-1$ | 1 | 1 | 0 | 0 | $-1$ | 1 |
| $c_{11}$ | 1 | $-1$ | $-1/2$ | $1/2$ | 1 | 1 | 1 | $-1$ |
| $c_{12}$ | 1 | $-1$ | $-1/2$ | $1/2$ | $-1$ | 1 | $-1$ | 1 |
| Symmetry | $S_x S_y$ | $S_x A_y$ | $S_x S_y$ | $S_x A_y$ | $A_x S_y$ | $A_x A_y$ | $S_x S_y$ | $S_x A_y$ |
| Point of BZ | $\Gamma$ | $M-0$ | $K_1$ | $K_2$ | $K_1$ | $K_2$ | $M+0$ | $D$ |

possible in those clusters in which the number of atoms $N$ is divisible by three. Since $N$ also has to be even, due to the equal number of atoms in sublattices A and B, the number $N$ finally has to be divisible by six. This is the base for rule 3 of cluster building from Section II.

It is easy to see that in clusters $N = 8, 10$ and other $N$ not divisible by six, energy values $\varepsilon = 0$ are absent. Therefore, only clusters with $N$ divisible by 6 must be taken into consideration in the case of endless layers.

## VI. NANORIBBONS AND NANOTUBES

The CC approach is especially applicable to impurities, as well as nanotubes and nanoribbons. In the latter two cases a group of atoms lying across the tubes or ribbons is a natural cluster, in which the number of atoms depends on the diameter of the tube or the width of the ribbon (Fig. 7). Let us now consider the armchair ribbon with $N = 12$. As zigzag nanoribbons are not analogous to carbon nanotubes [12], the former will not be discussed in this work. The above mentioned cluster is shown in (Fig. 7(b)). This cluster differs from the cluster in Fig. 2(b) in a single, yet very significant aspect: the cluster in Fig. 7(b) has no closing bonds between atoms 1–6 and 7–12. This reflects the fact that the latter atoms are situated on the edge and therefore are connected to the

ribbon by two, not three bonds.
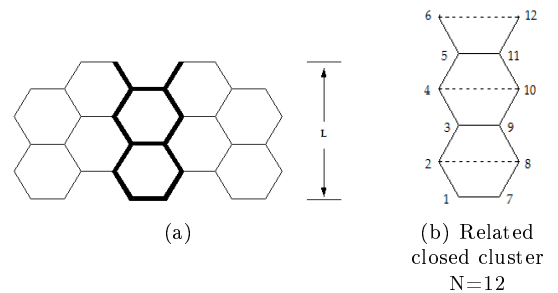


(a)

(b) Related closed cluster N=12

Fig. 7. Armchair ribbon (a) and the corresponding closed cluster $N = 12$ (b).

As one can see, the cluster in Fig. 7(b) belongs to a well known ladder type. The determinant $D_N$ of this cluster may be written in a block form for any even $N$

$$D_N = \begin{vmatrix} L_{N_1}(\varepsilon) & I_{N_1} \\ I_{N_1} & L_{N_1}(\varepsilon) \end{vmatrix}, \qquad (17)$$

where

$$N_1 = \frac{N}{2},$$

$$L_{N_1}(\varepsilon) = \left. \begin{vmatrix} \varepsilon & 1 & & & & & \\ 1 & \varepsilon & 1 & & & & \\ & 1 & \varepsilon & 1 & & & \\ & & & \cdot & & & \\ & & & & \cdot & & \\ & & & & & 1 & \varepsilon & 1 \\ & & & & & & 1 & \varepsilon \end{vmatrix} \right\} N_1 \qquad (18)$$

and $I_{N_1}$ being the unity matrix of order $N_1$.

The determinant (17) can be brought into a quasi-triangular form. For this, we need to add row number $(N_1 + 1)$ to the first row, row $(N_1 + 2)$ to the second, and so on until row $N_1$ is added to row $2N_1$. Then, the first column is subtracted from column $(N_1 + 1)$, second from $(N_1 + 2)$ and similarly column $N_1$ from $2N_1$.

As a result, we obtain

$$D_N = L_{N_1}(\varepsilon + 1)L_{N_1}(\varepsilon - 1), \qquad (19)$$

where $L_n(x)$ are well-known polynomials, expressions of which are given in [10] (for $g_n(x)$ there) for $n \le 20$. It is also known that the representation of $L_n(x)$ via the trigonometric functions is [11]

$$L_n(x) = \frac{\sin[(n + 1)\theta]}{\sin \theta}, \qquad (20)$$

where $x = 2\cos\theta$.

Then, for obtaining the energy values $D_N(\varepsilon) = 0$ is reduced to conditions which need to satisfy at least one of two of the following equations:

$$L_{N_1}(\varepsilon + 1) = 0 \qquad (21)$$

or

$$L_{N_1}(\varepsilon - 1) = 0. \qquad (22)$$

In view of (20), these equations lead to

$$\sin[(N_1 + 1)\theta_+] = 0 \qquad (23)$$

and

$$\sin[(N_1 + 1)\theta_-] = 0, \qquad (24)$$

where the $\theta_\pm$ are determined from

$$2\cos\theta_\pm = \varepsilon \pm 1. \qquad (25)$$

The solutions of (23) and (24) are

$$\theta_\pm = \frac{n_\pm \pi}{N_1 + 1}, \qquad (26)$$

where $n_\pm = 1, 2, \ldots, N_1$.

Then, from (25) we get the formula for the energy values of a closed cluster with $2N_1$ atoms, which describes the nanoribbon

$$\varepsilon_{n_\pm} = 2\cos\frac{n_\pm \pi}{N_1 + 1} \pm 1. \qquad (27)$$

Taking into account that $n_+$ and $n_-$ both may possess $N_1$ values and due to the $\pm 1$ part we see from (27) that $\varepsilon_{n_\pm}$ possesses $2N_1 = N$ values, as this has to be the case for a cluster with $N$ atoms.

If the ribbon is transformed into an infinite layer ($N_1 \to \infty$), then we get the boundary energy spectrum values from

(27), which are $\varepsilon_{\max} = 3$ at $n_+ = 1$ and $\varepsilon_{\min} = -3$ at $n_- = N_1$. These values also coincide with the result in section III.

Using equation (27), one can easily find the values of $N_1$, under which the solutions $\varepsilon_{n\pm} = 0$ exist, that is the ribbon is metallic. The condition for this is $\cos\frac{n_-\pi}{N_1+1} = \frac{1}{2}$ or $\cos\frac{n_+\pi}{N_1+1} = -\frac{1}{2}$, otherwise $\frac{n_-\pi}{N_1+1} = \frac{\pi}{3}$, $\frac{n_+\pi}{N_1+1} = \frac{2\pi}{3}$; $n_+ = 2n$. Denoting $n_- = M$, one can write both above equations as

$$N_1 = 3M - 1, \qquad (28)$$

with $M$ being an integer.

The formula (28) is the same as has been obtained using the tight binding model in [13] and [14].

The wave functions of nanoribbons with metallic conductivity can be found by using the symmetry, like it is done for the infinite layer in section V.

We consider as an example the case $N_1 = 5$. The closed clusters for the description of the ribbon are shown in figures 8(a) and 8(b). According to the graph theory terminology [6], these clusters are isomorphic to each other as well as to the ladder graph shown in Fig. 8(c). The energy spectra of these graphs are therefore the same.
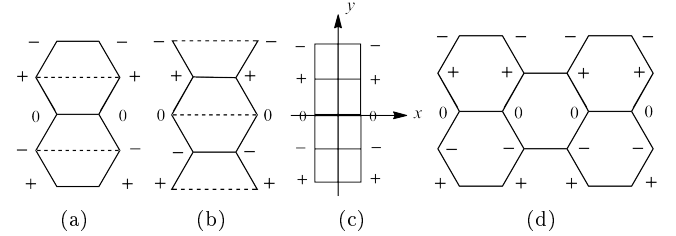
Fig. 8. Wave functions of clusters for description of ribbon $N_1 = 5$ (a,b), ladder cluster (c) and ribbon with symmetry $A_x S_y$ at $\varepsilon = 0$ (d)

Similar to the case of infinite layer, one can also obtain the energy values of the cluster, which corresponds to various symmetries. Results for $N_1 = 5$ are shown in Table 4.

If only the energy spectrum is required, it can be directly obtained from equation (27).

The cases for other $N_1$ can be considered likewise. Figure 9 shows the wave functions of the symmetry $A_x S_y$ for the $N_1 = 8$ ribbon at $\varepsilon = 0$.
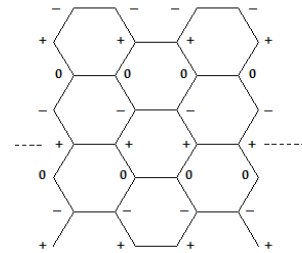
Fig. 9. Wave functions of symmetry $A_x S_y$ for the ribbon $N_1 = 8$ at $\varepsilon = 0$

If we compare the ribbons shown in Figures 8(d) and 9, we can see the meaning of the metallic conductivity condition (28): when increasing $N_1$, in order to keep the energies of each atom at zero, it is necessary to add two rows of atoms, with positive and negative $|p_z\rangle$. The latter must, however, be separated from the previous row by including a row of zeroes. Altogether, we need to add three rows, which is where the term $3M$ in (28) derives from. From Figures 8 and 9 one can also see that the distance between the nodes $\frac{\lambda}{2} = \frac{3}{4}a$ and the

Table 4. Energy spectrum of a closed cluster for description of a $N_1 = 5$ ribbon

| Symmetry | Energy | | | | | | | | | |
|---|---|---|---|---|---|---|---|---|---|---|
| $S_x S_y$ | $-\sqrt{3}-1$ | | $-1$ | | | | $\sqrt{3}-1$ | | | |
| $S_x A_y$ | | | | $-\sqrt{3}+1$ | | | | $1$ | | $\sqrt{3}+1$ |
| $A_x S_y$ | | $-2$ | | | $0$ | | | | | |
| $A_x A_y$ | | | | | | $0$ | | | $2$ | |

Table 5. The connection between the ribbon width $L$ (scaled by a), $N_1$ and $M$ in the case of metallic conductivity

| $M$ | $N_1$ | $L^{\mathrm{met}}$ |
|---|---|---|
| 1 | 2 | $^1/_2$ |
| 2 | 5 | 2 |
| 3 | 8 | $^7/_2$ |
| 4 | 11 | 5 |
| ... | ... | ... |

wave front is parallel to axis $x$. This corresponds to the wave vector $\boldsymbol{k}$ at point $K_1$ of the Brillouin zone. It is easy to see that in the case of the symmetry $A_x A_y$ the energy value $\varepsilon = 0$ corresponds to the point $K_2$, similar to the infinite layer.

Using $N_1$ is not the only way to describe the criterion for metallic conductivity. It also can be written using the width of the ribbon $L$. Figures 8(d), 9 and equation (28) show that it is possible to obtain the connection between $M$, $N_1$ and $L$ as in Table 5.

The relation between $L$ and $M$ in Table 5 can be written as

$$L^{met} = \frac{3M-2}{2}, \qquad M = 1, 2, 3 \dots . \qquad (29)$$

This formula differs from $L = 3M + 1$ in [15], which is maybe due to the different definition of the ribbon width in [15].

Figure 10 shows the dependence between the energy gap $\varepsilon_g$ and the ribbon width. Here, $\varepsilon = 2\varepsilon_1$, where $\varepsilon_1$ is the nearest level to zero and is found via (27).
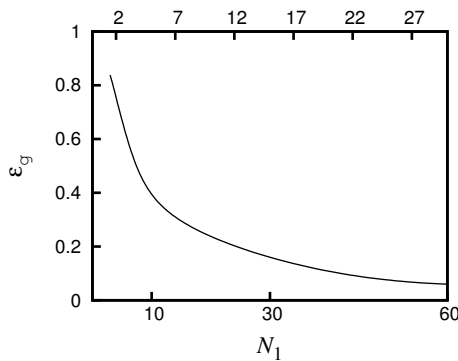
Fig. 10. Dependence between the energy gap $\varepsilon_g$ and the ribbon width

The values of $N_1$ and $L$, where $\varepsilon_g = 0$, are not marked, they can be obtained from equations (28) and (29).

The described approach of the calculation of nanoribbons using ladder clusters may also be applied to nanotubes, with some modifications. The formal transition from the nanoribbon to the nanotube consists in closing a cluster of the type shown in Fig. 7(b), so that the closing happens between atoms 1–6 and 7–12 — this way we get the cluster from Fig. 2(b). If we wrap it up into a cylinder form, we obtain a cluster with three hexagons. It can be easily verified that in clusters of this type the number of hexagons in the cylinder section is always an integer.

However, a cluster of the type as in Fig. 8 cannot be wrapped up in such a way, because the atoms of the upper and lower edge are from the same sublattice, A or B, and nearest neighbors always have to be from different sublattices.

Therefore, in order to wrap up a cluster into a cylinder, one must add a row of atoms. These atoms need to belong to a different sublattice than the atoms at the edges of the initial cluster. In the $N_1 = 5$ example, this means that the number $N_c$ of atoms situated along the circle cylinder section must equal six.

It may also be easily verified that for clusters of both types $N_c$ must be even (which is a consequence of the equal number of A and B atoms) and the number of hexagons $N_S$ along the circle has to be an integer. Here, beginning with the smallest value $N_s = 2$ it is $N_c = 2N_s$.

In the case of metallic conductivity ($\varepsilon_g = 0$) as well as in the infinite layer (section V), it is necessary for $N_c$ to contain an integer number of atomic triplets $+, -, 0$, that is, $N_c$ needs to be not only even but also divisible by three. All in all, $N_c$ has to be divisible by six, and therefore, we can write the criterion of metallic conductivity of nanotubes as

$$N_c^{\mathrm{met}} = 6M, \qquad M = 1, 2, 3 \dots . \qquad (30)$$

For all other values of $N_c$, there is $\varepsilon \neq 0$. For example, in the case of the least values $N_s = 2, N_c = 4$, one must consider the closed cluster $N = 8$. It is possible to calculate a cluster of type from Figure 2(b), but for $N = 8$.

Solving equation (4) for this case gives us the following energy spectrum:

$$\varepsilon^c = \pm 1, \pm 1, \pm 1, \pm 3. \qquad (31)$$

Hence, the value of the energy gap for $N_c = 4$ is $\varepsilon_g^c = 2$, which is the maximum value of $\varepsilon_g^c$ for nanotubes. With an increasing $N_c$ the value of $\varepsilon_g^c$ decreases.

It should be noted that $\varepsilon^c$ in (31) and $\varepsilon_g^c$ are scaled by $\gamma_0^c$: $\varepsilon_c = \frac{E_c}{\gamma_0^c}$, where $\gamma_0^c$ is the tube's transfer integral (hopping energy). This latter value is different from the value of $\gamma_0$ for the infinite layer and is dependent on $N_c$, which should be taken into the account when $\varepsilon_g^c$ in $eV$ needs to be obtained. However, this dependence does not exert any influence on the criterion $\varepsilon_g = 0$.

## VII.  IMPURITY IN GRAPHENE

The cluster approach is, as already mentioned, especially appropriate for studying impurities in crystals. This is connected with the fact that the impurity influence on the crystal depends mainly on the interaction with atoms which are located in the nearest environment of this impurity. Exactly those atoms together with the impurity are the ones which can be considered as a cluster with N atoms. The study of this cluster is the essence of the impurity problem in the present approach.

In this paper, we restrict the consideration to the simplest cluster $N = 6$. Let us assume that at the first lattice point of this cluster atom C is substituted with another one. This atom only differs from C in terms of the $|p_z\rangle$-electron energy of an isolated atom, which is $E_0 + \Delta E_0$ instead of just $E_0$. It is also assumed that this impurity atom is silicon, although is also might be germanium or any other atom with the same outer electron shell structure as C. Furthermore, we assume the transfer integral $\gamma_0$ equal between all neighboring atoms. In order to account for the difference in these parameters within the cluster approach, one simply has to replace the ones in the corresponding Hamiltonian matrix elements with parameters, which characterize the transfer integral between the impurity and the surrounding atoms. The issue of the influence of these parameters on the energy spectrum in 3D crystals has been investigated by us earlier using Green's functions [16]. For the purpose of this paper, however, this problem is not of a fundamental meaning, in so far as the main parameter is $\Delta E_0$.

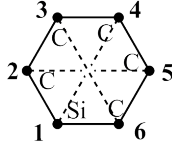An example of a closed cluster with one impurity atom Si is shown in Fig. 11.



Fig. 11. Closed cluster $N = 6$ with one impurity atom Si

The secular equation for this cluster has the form

$$
D_6 = \begin{vmatrix}
(\varepsilon - \Delta) & 1 & & 1 & & 1 \\
1 & \varepsilon & 1 & & 1 & \\
& 1 & \varepsilon & 1 & & 1 \\
1 & & 1 & \varepsilon & 1 & \\
& 1 & & 1 & \varepsilon & 1 \\
1 & & 1 & & 1 & \varepsilon
\end{vmatrix} = 0, \quad (32)
$$

where $\Delta = \frac{\Delta E_0}{\gamma_0}$.

This sixth degree equation is reduced to a cubic equation, which can be solved analytically. As a result we get the following solutions

$$\varepsilon_{1,2,3} = 0.$$

$$\varepsilon_{4,5,6} = \frac{1}{3}\left[\Delta + 2\sqrt{\Delta^2 + 27}\,\cos\left(\frac{\varphi}{3} + n\frac{2\pi}{3}\right)\right], \quad (33)$$

$$n = 0, 1, 2\ldots$$

where

$$\cos\varphi = \frac{\Delta\left(\Delta^2 - \frac{3^4}{2}\right)}{(\Delta^2 + 27)^{\frac{3}{2}}}. \quad (34)$$

It is easy to see that under $\Delta = 0$ there is

$$\varepsilon_4^0 = 3, \varepsilon_5^0 = -3, \varepsilon_6^0 = 0,$$

that is we obtain the result (6).

The numerical calculations of the dependence of $\varepsilon$ on $\Delta$, which may be obtained from (33) and (34) or, simpler, directly from the calculation of the determinant (32), are shown in Figure 12.
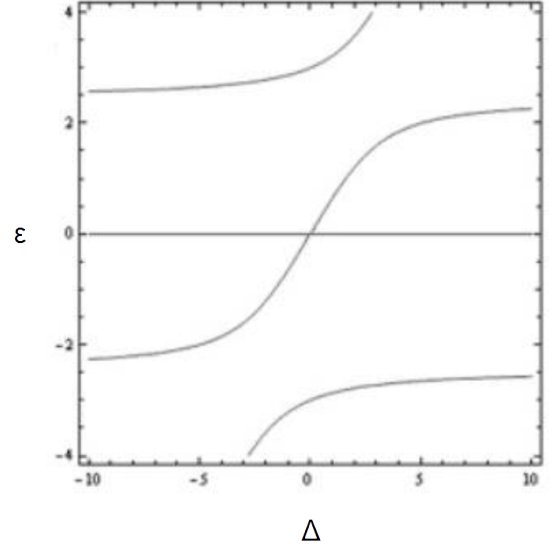


Fig. 12. Dependence of energy levels of cluster $N = 6$ on $\Delta$. The level $\varepsilon = 0$ is threefold degenerated

As one can see, we get a result which is typical of the perturbation process: the fourfold degenerate level $\varepsilon = 0$ splits partially and the non-degenerate level moves. At the same time, level $\varepsilon = 0$ still remains threefold degenerate. That is why there is no arising gap between the valence and conduction bands. The level which is split from the originally fourfold degenerated level $\varepsilon = 0$ is the impurity level in the conduction band, that is the resonance level.

## VIII.  THE ENERGY BANDS OF MONOATOMIC LAYER $C_{1-x}Si_x$ ($0 \leq x \leq 1$)

Using the CC approach, one may as well calculate the energy spectrum of a hypothetical object, a monoatomic layer of the type $C_{1-x}Si_x$. That such an object can be created results from the following reasoning: when obtained by means of epitaxi, graphene can be formed on the surface of SiC. The monolayer of Si, which appears here as a buffer layer, has also a hexagonal structure [17]. That is why by means of epitaxi, perhaps not only graphene can be formed but also the monoatomic layer of the type $C_{1-x}Si_x$ ($0 \leq x \leq 1$), with a hexagonal structure similar to graphene.

In the study of this problem, we restrict ourselves to considering only the simplest structure $N = 6$. This is found to be sufficient for outlining the energy band structure of $C_{1-x}Si_x$.

We consider the cases separately when in a cluster of 6 C-atoms one, two, three, four or five atoms are replaced with Si-atoms. This corresponds to the values $x = \frac{1}{6}; \frac{1}{3}; \frac{1}{2}; \frac{2}{3}; \frac{5}{6}$, respectively. The case of $x = \frac{1}{6}$ has been already considered in the previous section. It should be noted that by "impurity" we mean the atoms which are present in a lesser number. That

is at $x = \frac{1}{3}$ the impurity atoms are those of Si and at $x = \frac{2}{3}$ those of C.

The clusters corresponding to these $x$-values can be of two types. Namely, for $x = \frac{1}{3}$ two impurity Si-atoms can interact with each other (type II) or not interact (type I). The same can be obtained for C-atoms for $x = \frac{2}{3}$. First, we study the clusters of type I, which are shown in Fig. 13.
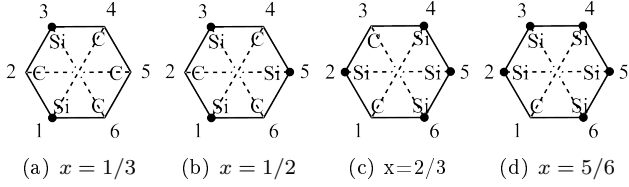


(a) $x = 1/3$    (b) $x = 1/2$    (c) x=2/3    (d) $x = 5/6$

Fig. 13. Clusters of type I with $N = 6$ for $C_{1-x}Si_x$

The secular equations for clusters shown in Fig. 13 can easily be estimated. For example, for $x = \frac{1}{3}$ we obtain

$$\begin{vmatrix} (\varepsilon - \Delta) & 1 & & 1 & & 1 \\ 1 & \varepsilon & 1 & & 1 & \\ & 1 & (\varepsilon - \Delta) & 1 & & 1 \\ 1 & & 1 & \varepsilon & 1 & \\ & 1 & & 1 & \varepsilon & 1 \\ 1 & & 1 & & 1 & \varepsilon \end{vmatrix} = 0. \quad (35)$$

For other values of $x$, the equations have a similar form. In all cases, the equations of the sixth degree are to be reduced to equations of the third degree and are solved analytically.

The results of these calculations are:

$$x = \frac{1}{3}: \qquad \varepsilon_{1,2} = 0; \ \varepsilon_3 = \Delta,$$

$\varepsilon_{4,5,6}$ are determined by formula (33), but with other $\varphi$, namely

$$\cos\varphi = \frac{\Delta^3}{(\Delta^2 + 27)^{\frac{3}{2}}}. \quad (36)$$

$$x = \frac{1}{2}, \quad (SiC):$$
$$\varepsilon_{1,2} = 0;$$
$$\varepsilon_{3,4} = \Delta; \quad (37)$$
$$\varepsilon_{5,6} = \frac{\Delta \pm \sqrt{\Delta^2 + 36}}{2}.$$

$$x = \frac{2}{3}: \qquad \varepsilon_1 = 0;$$
$$\varepsilon_{2,3} = \Delta;$$
$$\varepsilon_{4,5,6} = \frac{2}{3}\left[\Delta - \sqrt{\Delta^2 + 27} \ \cos\left(\frac{\varphi}{3} + n\frac{2\pi}{3}\right)\right];$$
$$n = 0, 1, 2 \ldots$$
$$\quad (38)$$

where $\varphi$ is the same as in (36)

$$x = \frac{5}{6}: \qquad \varepsilon_{1,2,3} = \Delta;$$
$$\varepsilon_{4,5,6} = \frac{2}{3}\left[\Delta + \sqrt{\Delta^2 + 27} \ \cos\left(\frac{\varphi}{3} + n\frac{2\pi}{3}\right)\right];$$

where

$$\cos\varphi = \frac{\Delta(\Delta^2 - \frac{1}{2}3^4)}{(\Delta^2 + 27)^{\frac{3}{2}}};$$
$$n = 0, 1, 2 \ldots$$
$$\quad (39)$$

The dependence of the energy bands of $C_{1-x}Si_x$ on $x$ is shown in the form of a diagram in Fig. 14. This diagram is obtained from formulas (33), (34), (36)–(39) for $\Delta = 3.5$, which corresponds roughly to the value of $\Delta$ for Si in graphene.
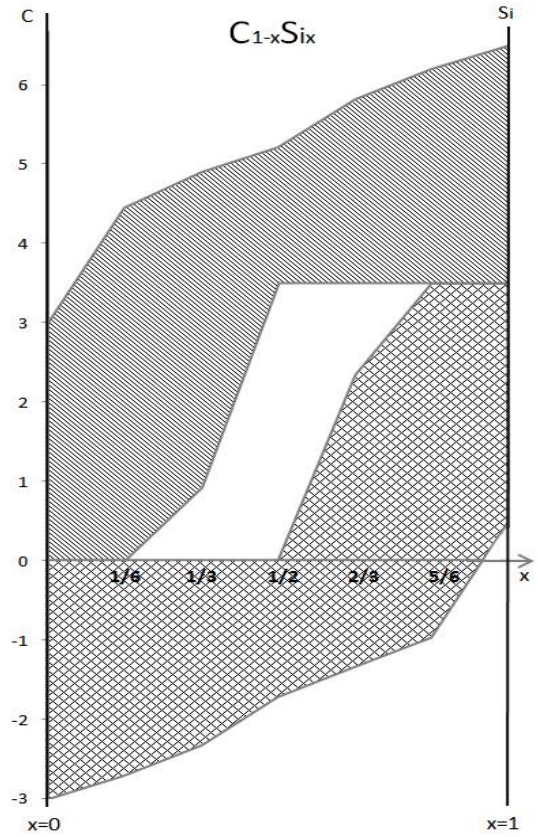


Fig. 14. Energy spectrum of the mono-atomic layer $C_{1-x}Si_x$. checkered: valence band; striped: conduction band; plain: forbidden band

The main feature of this band structure arises from a forbidden band with the typical tunnel form. From this one can suggest that in principle it is possible to create a tunnel diode on the basis on a $C_{1-x}Si_x$ layer. In the ground of such a diode can be a tunnelling between Si- and C-domains of the layer in which the concentration of $x$ changes with the coordinate $x$. That is, if in Fig 14 $x$ is not only the concentration, but also the coordinate $x$.

Next we study the clusters of type II, in which impurity atoms interact not only with basic atoms of the layer but also with each other. The latter is possible, if the impurities are at the lattice points of a different sublattice: A and B, because the atoms of the same sublattice do not interact with each other in the nearest neighbors approximation.

In the case of $x = \frac{1}{3}$, the cluster of type II can be obtained from the cluster in Fig. 13(a), if we place the atoms Si at the lattice points, for example 2 and 5 instead of 1 and 3. C-atoms with $x = \frac{2}{3}$ in the cluster in Fig. 13(c) can be treated the same way. As a result, we obtain the following solutions for clusters of type II:

$$
x = \frac{1}{3} : \qquad \varepsilon_{1,2} = 0;
$$

$$
\varepsilon_{3,4} = \frac{1}{2}\left(\Delta - 3 \pm \sqrt{\Delta^2 + 2\Delta + 9}\right);
$$

$$
\varepsilon_{5,6} = \frac{1}{2}\left(\Delta + 3 \pm \sqrt{\Delta^2 - 2\Delta + 9}\right). \tag{40}
$$

$$
x = \frac{2}{3} : \qquad \varepsilon_{1,2} = \Delta;
$$

$$
\varepsilon_{3,4} = \frac{1}{2}\left(\Delta - 3 \pm \sqrt{\Delta^2 - 2\Delta + 9}\right);
$$

$$
\varepsilon_{5,6} = \frac{1}{2}\left(\Delta + 3 \pm \sqrt{\Delta^2 + 2\Delta + 9}\right). \tag{41}
$$

From formulas (40) and (41) one can obtain the energy of impurity states, which at $\Delta = 3.5$ can be found mostly within valance and conduction bands. The single level which can be found in the forbidden band appears when $x = \frac{1}{3}$. This level can take part in tunnelling, which we discussed above.

## IX. CONCLUSIONS

In this paper, the CC approach has been applied to some problems of the calculation of the grpahene energy spectrum. This approach seems to be especially appropriate both for problems of the breach of the graphene's periodical structure (point defects, boundaries) and for problems besides monolayer graphene (bilayer graphene, compound $C_{1-x}Si_x$).

As for the precision of the approach, it may easily be increased by considering clusters of larger sizes and their interaction not only with the nearest neighbors. Besides, it is not difficult to study a cluster with a distortion of the lattice near the point defect. One can also consider the conglomerates of point defects in a graphene lattice.

Except various problems with the calculation of the electron energy spectrum, the closed cluster approach may as well be applied to calculate the vibration spectrum in graphene, like as it is done for one-dimensional and three-dimensional crystals in [18], [19].

## X. ACKNOWLEDGMENTS

[1] K. Wakabayashi, in *Graphene Nanoelectronics: Metrology, Synthesis, Properties and Applications*, edited by Hassan Raza (Springer, Berlin–Heidelberg, 2012), p. 277; https://doi.org/10.1007/978-3-642-22984-8_9.

[2] I. I. Tal'yanskij, Fiz. Elektron. **28**, 8 (1984).

[3] M. Lannoo, J. Bourgoin, *Point Defects in Semiconductors. I. Theoretical Aspects* (Springer, Berlin–Heidelberg, 1981); https://doi.org/10.1007/978-3-642-81574-4.

[4] A. K. Geim, K. S. Novoselov, Nat. Mat. **6**, 183 (2007); https://doi.org/10.1038/nmat1849.

[5] P. R. Wallace, Phys. Rev. **71**, 622 (1947); https://doi.org/10.1103/PhysRev.71.622.

[6] N. Trinajstić, *Chemical Graph Theory* (CRC Press, Boca Raton, Florida, 1983), Vol. I.

[7] E. Heilbronner, H. Bock. *The HMO Model and its Application* (Wiley & Sons Verlag Chemie, Weinheim, 1976).

[8] A. H. Castro Neto, F. Guinea, N. M. R. Peres, K. S. Novoselov, A. K. Geim, Rev. Mod. Phys. **81**, 109 (2009); https://doi.org/10.1103/RevModPhys.81.109.

[9] T. Seyller, Phys. J. **9**(8/9), 53 (2010); https://www.pro-physik.de/restricted-files/100121.

[10] T. Au-Chin, K. Yuan-Sun, Y. Guo-Sen, T. Shu-San, *Graph Theoretical Molecular Orbitals* (Science Press, Beijing, China, 1986).

[11] I. O. Vakarchuk, *Quantum Mechanics*, 3rd edition (Lviv University Press, Lviv, 2007).

[12] K. Wakabayashi, K. Sasaki, T. Nakanishi, T. Enoki, Sci. Technol. Adv. Mater. **11**, 054504 (2010); https://doi.org/10.1088/1468-6996/11/5/054504.

[13] M. Fujita, K. Wakabayashi, K. Nakada, K. Kusakabe, J. Phys. Soc. Jap. **65**, 1920 (1996); https://doi.org/10.1143/JPSJ.65.1920.

[14] K. Nakada, M. Fujita, G. Dresselhaus, M. Dresselhaus, Phys. Rev. B **54**, 17954 (1996); https://doi.org/10.1103/PhysRevB.54.17954.

[15] L. Brey, H. A. Fertig, Phys. Rev. B **73**, 235411 (2006); https://doi.org/10.1103/PhysRevB.73.235411.

[16] I. I. Tal'yanskij, B. L. Yudanin, Fiz. Tv. Tela **19**, 3040 (1977).

[17] B. Trauzettel, Phys. J. **6**(7), 39 (2007); https://www.pro-physik.de/restricted-files/110496.

[18] I. I. Talyansky, J. Phys. Stud **1**, 106 (1996); https://doi.org/10.30970/jps.01.106.

[19] I. I. Talyansky, A. T. Maksymov, J. Phys. Stud. **1**, 564 (1997); https://doi.org/10.30970/jps.01.564.

# ЗАСТОСУВАННЯ ПІДХОДУ ЗАКРИТОГО КЛАСТЕРА ДО ҐРАФЕНУ

Ілля І. Тальянський

*Кафедра теоретичної фізики, Львівський національний університет імені Івана Франка;*
*поточна адреса[†]: Rudolf-Breitscheid-Strasse 39, 23968, Wismar, Germany*
[†]Ми публікуємо цю статтю з нагоди 95-річчя покійного професора Іллі Тальянського (1928–2018). Ориґінальна версія з'явилася 2015 року як препринт https://arxiv.org/abs/1508.05385 і досі не опублікована. Коротку біографічну довідку про проф. Тальянського подано нижче.

Метод закритого кластера (метод ЗК) використовують для пошуку розв'язків різноманітних задач розрахунку енерґетичної зонної структури ґрафену. Суть методу ЗК полягає в додаванні до звичайного кластерного методу замикання зв'язків між крайовими атомами для усунення "обвисаючих" зв'язків на краях кластера. Ми вивчаємо випадки "нескінченного" шару ґрафену, а також нанострічок, нанотрубок і двошарового ґрафену. Результати для цих випадків узгоджуються з тими, що були отримані за допомогою інших методів (апроксимація жорсткого зв'язку та інші). За допомогою методу ЗК ми також досліджуємо проблему точкових дефектів у ґрафені та отримуємо спотворення енерґетичного спектра. Знайдено енерґетичний спектр шару $C_{1-x}Si_x$ ($0 \leq x \leq 1$), а також залежність ширини забороненої зони від концентрації кремнію. Ми показуємо, що енерґетична зонна структура $C_{1-x}Si_x$ виглядає як тунельний перехід. Також отримано хвильові функції ґрафену в точках симетрії зони Бріллюена.

**Ключові слова:** ґрафен, енерґетична зонна структура, точкові дефекти, наноструктури.

## ILLYA TALYANSKY (1928–2018): BIOGRAPHICAL NOTE



**Illya TALYANSKY** or **Ilja TALJANSKIJ** (**Ілля ТАЛЬЯНСЬКИЙ**, 04 July 1928 in Tal'ne, Cherkasy reg., Ukraine – 20 January 2018 in Wismar, Mecklenburg-Vorpommern, Germany) was a theoretical physicist.

He was born in the town of Tal'ne, Cherkasy region of Ukraine. During the Second World War, the family was evacuated to Siberia, where Illya Talyansky finished school. After the war, the family moved to Lviv, where he entered the Physics and Mathematics Faculty of the University of Lviv. He completed his studies in 1950 and his postgraduate studies in 1953. On 16 February 1954, he defended his Candidate of Sciences dissertation *Энергия и мезонные потенциалы в теории с высшими производными [Energy and meson potentials in a theory with higher derivatives]* at the University of Lviv (scientific supervisor Vasyl Milianchuk / Wasyl Milianczuk).

From 1954 to 1958, Illya Talyansky held the position of Senior Lecturer, and from 1958 to 1964, he served as an Associate Professor (Docent) at the Department of Physics at Lviv Agricultural Institute. From 1964 to 1970, he was an Associate Professor at the Department for Solid State Theory of the University of Lviv. From 1970 to 1995, Illia Talyansky was an Associate Professor and from 1995 to 1998, he held the position of Professor at the Department for Theoretical Physics of the University of Lviv.
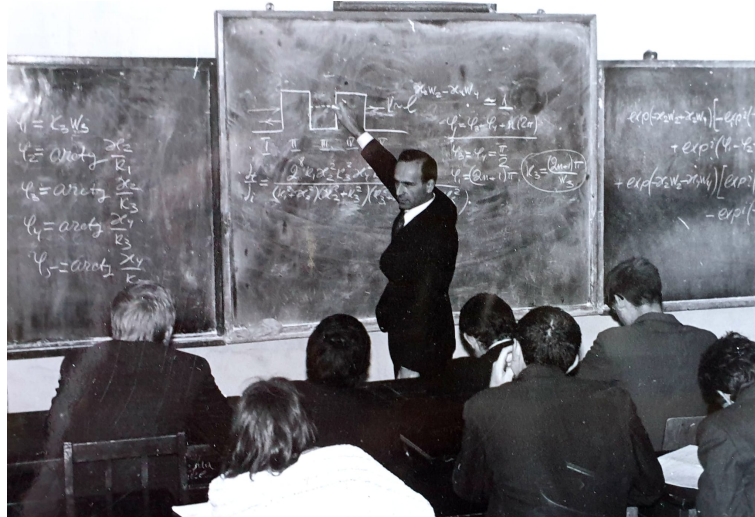


On 09 February 1994, he defended his Doctor of Sciences dissertation *Процеси переносу електронів і нейтронів у неоднорідних середовищах [Electron and neutron transfer processes in heterogeneous media]*. Upon retiring in 1998, Professor Talyansky moved to Wismar, Mecklenburg-Vorpommern, Germany. There, he continued to engage in research privately. Professor Talyansky also became a member of the German Physical Society (Deutsche Physikalische Gesellschaft). Already being in Germany, he maintained connections and continued to take interest in the life of his Department and University.

His scientific interests encompassed the theory of tunneling, the study of defects in solids, and the physics of narrow-band semiconductors. Professor Talyansky authored about 50 works.